Investigation of Commercial Tungsten Carbide as an HER Electrocatalyst in PEMWE

Xiaofeng Xie, Lanshan Liu, Shusheng Chen, Yuanquan Zhou, Xiaohong Hu[*]

Hubei Key Lab of Electrochemical Power Source, College of Chemistry and Molecular Sciences, Wuhan University. Wuhan Hubei, 430072, China
[*]E-mail: xhhu88@whu.edu.cn

Proton electrolyte membrane water electrolysis (PEMWE) is a promising hydrogen generation method limited by the high cost, such as those costs associated with noble electrocatalysts. Herein, we investigate commercial tungsten carbide (WC), a potential substitute for Pt, as a hydrogen evolution reaction (HER) electrocatalyst in PEMWE. We adopted two sizes of WC, 400 nm and 1 μm, optimized the electrode fabrication method and running conditions. The results show that the smaller WC does not provide stable performance and operating at high current density and low temperature is more competitive with Pt-based electrolysis. In addition, the most serious drawback is the increased cell voltage on restart after long-term power-off due to considerable WC oxidation, which leads to a decrease in the catalytic carbide carbon. Luckily, this can be offset by effective O_2 isolation in the cathode, such as H_2O sealing or pumping with H_2. WC is an economic alternative as a HER electrocatalyst in PEMWE with optimized conditions and an O_2 isolation strategy during an interrupted operation. We provide a practical method to reduce the cost of the HER electrocatalyst.

1. INTRODUCTION

Proton exchange membrane water electrolysis (PEMWE) has been attractive to green energy since the development of solid polymer electrolytes (SPEs) in the 1960s by General Electric [1, 2]. Compared with traditional water electrolysis, alkaline water electrolysis and solid oxide electrolysis, PEMWE rapidly develops because of higher efficiency, higher gas purity, and safer operation [3-5]. Despite the great potential of clean energy, the high cost of using noble metals as electrocatalysts and special frame materials limits its application. There are few choices for anodic electrocatalysts due to the high oxidation potential and acidic environment [6-8]. Hydrogen evolution reaction (HER)

electrocatalysts have a relatively broad selection. There has been significant research and development on platinum group metals (PGMs) and non-PGM electrocatalysts. With the exception of Pt loading reduction, developing non-precious electrocatalysts is a practical method to cut costs [3, 5]. One promising non-noble metal candidate is tungsten (W) and its compounds. According to a summary by Miles et al. [5], W shares a closed state with Pt, which means that it can be an ideal alternative for Pt in PEMWE.

Tungsten carbide (WC) has been known as "Pt-like" since Levy and Boudart [9] found it in 1976. Hence, numerous reports have been combined to investigate WC or its modified forms for methanol oxidation reactions [10-13], oxygen reduction reactions [14-16] and HER [17, 18]. Armstrong et al. [19] and Harnisch et al. [18] found WC had the highest activity, as compared to W_2C, WO_3, and WO_2. The catalytic ability reached 57% at neutral pH, and 31% in acidic conditions. Composite WC compounds have been shown to be more favorable. MoS_2/WC/RGO was synthesized by Yan et al. [20]; it showed excellent activity for positive synergistic effects and an improved electrical conductivity. Also, Ag-W_2C/C and Pt-WC/C were shown as low-cost and highly efficient electrocatalysts for ORR [21, 22]. Esposito et al. [17, 23] gave a detailed discussion on monolayer (ML) Pt, Pd, and Au on a WC substrate and indicated that ML Pt-WC showed comparable HER activity to bulk Pt. Except the various forms of WC and its composites, other methods have been applied to improve the electrocatalyst activity. The approach of creating more active sites displays a remarkable improvement in HER activity [24-27]. Also, synthesizing WC at an appropriate temperature along with hydrogen exposure builds a more effective surface carbon structure[28, 29]. In addition, high temperature PEMWE (HTPEMWE) is favorable based on the activation energy and kinetics of the reaction [30].

The extraordinary potential of WC for HER is generally accepted [31-34]. However, the aforementioned reports focus on synthesizing high activity WC or WC-based electrocatalysts. Most of those electrocatalysts still involve PGM loading or complex synthetic methods, which will bring extra costs to the electrocatalyst preparation. In addition, the electrochemical characterization of WC is conducted on a three-electrode system and cannot present a realistic situation in an integrated electrolyzer. In this paper, we adopted commercial WC as an HER electrocatalyst in PEMWE, summarized the optimal operating conditions for the WC electrode, and provided practical utilization of WC for PEMWE.

2. MATERIALS AND METHODS

2.1 WC electrode preparation

A WC electrode was fabricated by the decal transfer method [35]. WC ($\leq 1\mu m$, Shanghai Macklin Biochemical Co. Ltd, China) or WC (400 nm, Aladdin Industrial Corporation, USA), polytetrafluoroethylene (PTFE) suspension (wt. 60%) with or without purchased CFx (a hydrophobic agent, Hubei Zhuoxi Fluorochemical Co. Ltd, China), and isopropanol were mixed as a paste. The paste was repeatedly rolled on a clean PTFE sheet. Then it was transferred to a 3 cm x 3 cm carbon paper. After that, Nafion solution (wt. 5%, E. I. Du Pont Company, USA) was brushed on the surface of the fabricated WC electrode. Finally, the electrodes were dried at 130 °C in air (1 h) or at 60 °C in vacuum

(12 h) twice, the first time was to evaporate the solvent in the catalyst layer and the second time was to evaporate the solvent used for Nafion. Two hydrophobic agent compositions were compared, 10% PTFE and 3% PTFE with 7% CFx. Electrodes were made with different Nafion loadings (1.3, 1.8, 2.4, 3.0 mg cm^{-2}) and WC loadings (35.6, 46.7, 57.8 mg cm^{-2}).

2.2 Characterization of the WC electrode

2.2.1 Surface characterization of the WC electrode

Scanning electron microscopy (SEM, SUPRA 55, ZEISS, Germany), X-ray photoelectron spectrometry (XPS, ESCALAB250Xi, Thermo Fisher Scientific, USA) and energy dispersive X-ray Detection (EDX, X-MaxN, Oxford, England) were introduced to detect the surface parameters of the WC electrodes.

2.2.2 Performance of the WC electrode

The fabricated WC electrode was assembled with an H$^+$-exchanged Nafion$^®$-117 (E. I. Du Pont Company, USA) membrane and an anode as described in our previous work [36]. The Nafion membrane was first boiled in 10% H$_2$O$_2$ at 80 °C for 30 min. Then it was transferred to 2 mol L^{-1} H$_2$SO$_4$ at 80 °C for 30 min. Hot water washing was used until the water was neutral. Next, the well treated membrane was soaked in ultrapure water. The anode was composed of an IrO$_2$ catalyst layer (containing 80% IrO$_2$, 5% PTFE, and 15% Nafion. IrO$_2$ loading was 5 mg cm^{-2}) and a Pt-Sn-Sb coated porous Ti plate. A current collector and flow field plate were made of a Pt-coated Ti material. The PEM water electrolyzer was operated by a DC power supply at room temperature with a current density of 1 A cm^{-2}, and ultrapure water (18.2 MΩ cm) was fed to the anode side or both sides, as shown in Figure 1.
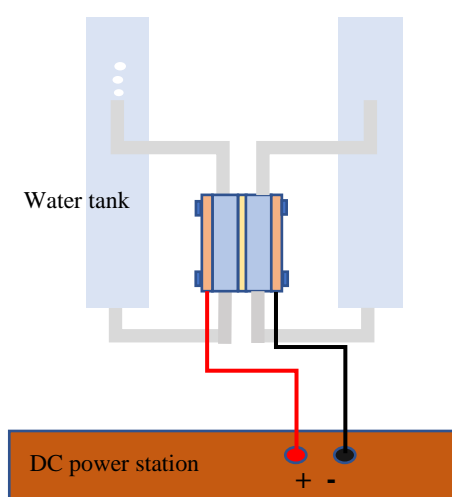

Figure 1. Water electrolysis schematic.

3. RESULTS AND DISCUSSION

3.1 Effect of WC size

The electrode composed of 400 nm-sized WC suffered serious oxidation and dissolution. The dissolution even occurred before running, as Figure 2 shows. After operation, the cell voltage and temperature quickly increased. This shows that the 400 nm WC is unsuitable for an integrated electrolyzer, though the smaller size promised more surface active area [27, 37]. It is necessary to characterize nano-size electrocatalysts in an electrolyzer system, not only in a three-electrode system. Most reports have no data when used in an electrolyzer. Considering this situation, only the 1-µm-sized WC was characterized (Figure S1) and used for the remaining experiments.

Figure 2. Pictures of 400 nm-size WC electrodes.

3.2 Effect of electrode fabrication

The electrode is the site of the electrochemical reaction. Reasonable electrode fabrication methods and electrode components typically guarantee higher performance for low energy consumption and catalyst loading [38, 39]. The catalyst coated membrane method proved to have higher performance than that of the gas diffusion electrode (GDE) method due to the improved proton connection [40]. However, the size of the WC was too big to be uniformly dispersed as a homogeneous catalyst ink, and, therefore, the traditional GDE method was applied to fabricate the WC electrode. For the WC electrode, WC works as an electron transfer medium, Nafion takes responsibility for proton transport, and a hydrophobic agent provides the gas channels. Herein, we investigated the factors of solvent removal, hydrophobic agent composition, Nafion loading, and WC loading on the performance of the WC electrode. The results are shown in Figure 3.
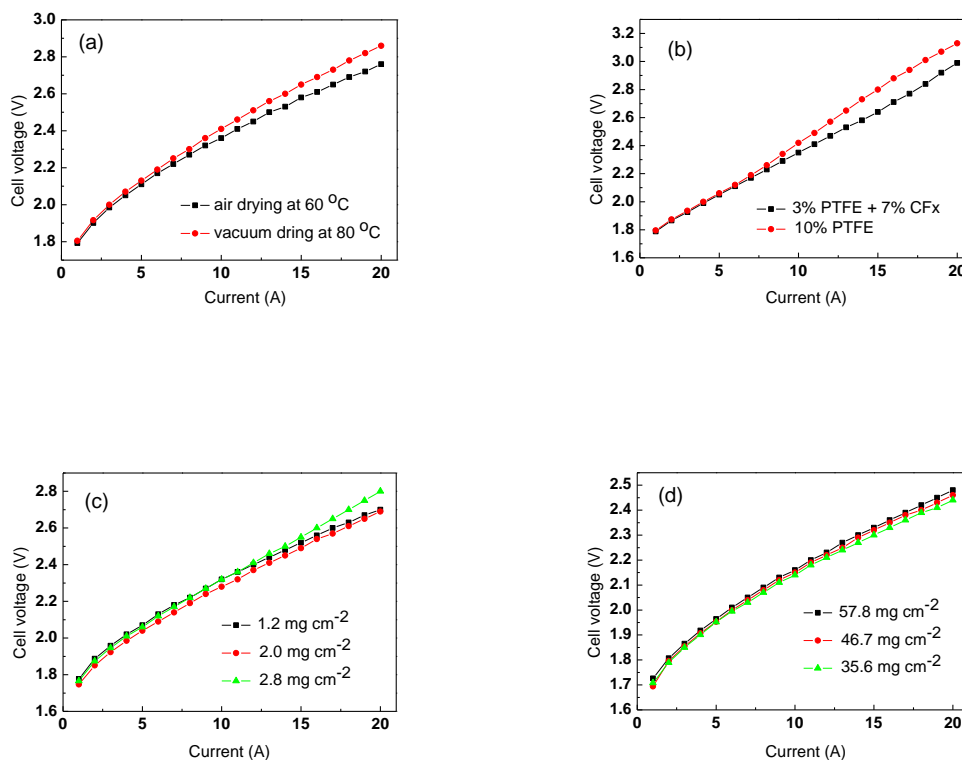
Figure 3. Polarization curves. (a) Polarization curves of the WC electrode with vacuum drying at 80 °C and air drying at 60 °C. Polarization curves were tested at 40 °C. (b) Polarization curves of the WC electrode with different hydrophobic agent compositions. Polarization curves were tested at 50 °C. (c) Polarization curves of the WC electrode (WC loading: 0.54 mg cm^{-2}) with different Nafion loading. Polarization curves were tested at 60 °C. (d) Polarization curves of the WC electrode (Nafion loading: 1.8 mg cm^{-2}) with different WC loading. Polarization curves were tested at 60 °C.

3.2.1 Effect of solvent removal method

We compared two solvent removal methods, vacuum drying at low temperature and air drying at a relatively high temperature. The results (Figure 3(a)) showed that the electrode fabricated by vacuum drying had a higher cell voltage than that of air drying, inconsistent with our expectation that vacuum drying would show a lower cell voltage. WC is unstable and easily oxidized, and vacuum drying at low temperature reduces the risk of oxidization [30]. While the results indicate oxidization during this process seems to be advantageous, the electrochemical activity of WC is questionable. Böhm thought that suitable oxidation contributes to the activity of the WC, and recently, the WC has shown no poor activity [11]. However, this hypothesis contrasts with later experiments. Thus, we believe the advantage of air drying is related to other phenomena. Vacuum drying requires long time to remove isopropanol, and the organic solvent might re-absorb on the porous electrode, providing insufficient solvent removal. In contrast to Pt/C, WC acting as the electrocatalyst does not need aqueous hydration, so only

isopropanol was used as the solvent. Isopropanol can be easily and quickly removed at 130 °C. WC oxidation is moderate at short-term O_2 exposure and high temperatures without water present.

3.2.2 Effect of hydrophobic agent composition

Despite sharing a similar weight ratio of 10% of the hydrophobic agent, the utilization of a composite hydrophobic agent shows advantages at high current densities, as shown in Figure 3(b). In using PTFE as a binder and hydrophobic agent, its ratio impacts the electrode structure and performance. Proper content of the hydrophobic agent establishes a reasonable balance of gas transport and electrical resistance [41]. 3% PTFE is adequate for particle bonding but not enough to build connective gas channels, while 10% PTFE leads to higher electrical resistance. Different from polymer PTFE, CFx can be easily and uniformly dispersed based on its powdered state, and the electron transport is less influenced. Thus, in the composite, PTFE was used as a binder and CFx as the hydrophobic agent.

3.2.3 Effect of Nafion and WC loading

According to the results (Figure 3(c)), the relationship between performance and Nafion loading showed a volcano trend. Low Nafion loading cannot create a successful proton channel between the membrane and catalyst layer High Nafion loading shows a much higher electrical resistance [42]. Moreover, in these experiments we brushed the Nafion solution on the electrode surface. Adding Nafion in the catalyst paste increased the challenges in the electrode fabrication. A thin film electrode was preferred, as shown in Figure 3(d). The active area of the WC electrode is a thin layer next to the membrane. Thicker CLs typically lead to higher electrical resistance and longer gas transport [37].

3.3 Effect of operating parameters

3.3.1 Effect of temperature and current density

Figures 4(a) and 3(b) show the polarization curves of the WC and Pt/C electrodes (Pt loading: 0.2 mg cm^{-2}), respectively, at 40 °C, 60 °C, and 80 °C. Figure 4(c) illustrates the cell voltage difference (ΔU) between the Pt/C electrode and WC electrode at different currents and temperatures. The WC electrode seemed to be competitive at high current density operation and low temperature.

Cell voltage can be expressed as Eq. (1):

$$E_{cell} = E_a^\theta + \eta_a - E_c^\theta + \eta_c + iR \qquad (1)$$

R represents the total resistance of electron, mass and proton transfer [43]. Electron transfer is supported by the electrocatalyst, mass transportation is more affected by the pore structure of three-phase boundaries, and proton migration is related to Nafion distribution and temperature [39]. The characterization of WC (Figure S1(3)) showed higher HER activity at high temperatures. This indicates better performance. However, high temperature also enables higher oxygen dissolution in water and accelerates the rate of O_2 crossover, increasing the chance of WC oxidation. Oxidized WC shows worse HER activity and electron conductivity compared to WC [26]. When running at high current density,

high purity hydrogen is uninterruptedly generated in the cathode side. It provides a protective condition and even partially recovers the oxygenated WC [29]. High current density also means higher H_2 pressure, which decreases oxygen dissolution. In addition, there is another benefit of high current density operation. No extra heat is needed because the heat generated by the internal resistance can warm the electrolyzer to 40-60 °C. To summarize, the WC electrode running at high temperature is good for higher activity while negative for stability and operating at high current density is advantageous to the overall stability and heat supply.
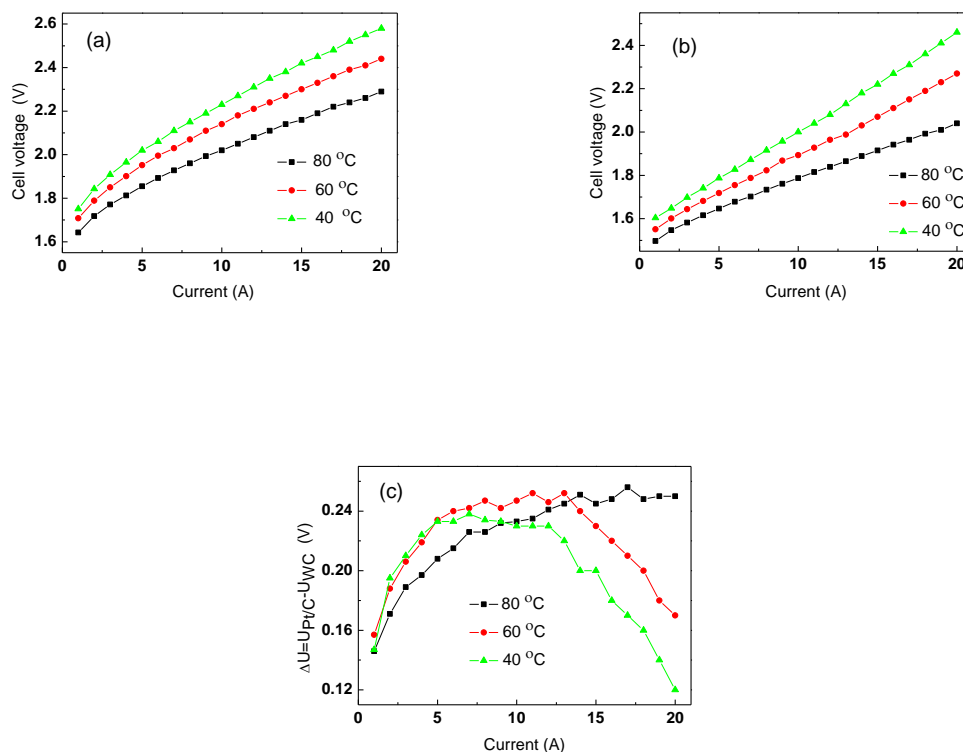

Figure 4. Polarization curves. (a) Polarization curves of the WC electrode at 40 °C, 60 °C, and 80 °C. (b) Polarization curves of the Pt/C electrode (Pt loading 0.2 mg cm^{-2}) at 40 °C, 60 °C, and 80 °C. (c) Cell voltage difference between the Pt/C electrode and WC electrode at different current and temperature.

3.3.2 Effect of cathode feeding water

The cell voltage showed a 30 mV differential between water supply and no water supply at the cathode side. After draining the cathode supply water, cell voltage immediately decreased 30 mV. Without water supply at the cathode, more heat can be utilized to warm the electrolyzer, which means the actual temperature of the electrolyzer increases. It also avoids O_2 dissolving in water.

3.4 Effect of power-off and repair strategy

3.4.1 Effect of power-off

There are flaws with the WC electrode. It suffers an unrecoverable performance loss after long times of being powered down. Short-time off-electrolysis can be mostly self-recovered by the restart operation, while it is workless for a long-time shut-down, shown in Figure 5. Further, the cell voltage even shows a slight decrease if electrolysis is interrupted by 15 min.

Figure 6 shows the surface of the WC electrode after it has stopped running. There were no significant differences between the new electrode (Figure S2) and used electrode (Figure 6(c) and 6(d)). However, if the used electrode stopped electrolysis for 15 days, the surface was gradually covered by bulky and yellow oxidized WC, as shown in Figures 6(a) and 5(b), which indicated serious oxidization. It is believed that the oxidization would be more serious with a longer power-off time. Bara WC is unstable, especially in acidic and anodic conditions. Thus, many papers only report WC as a support for noble electrocatalysts rather than as an electrocatalyst [14, 33]. When electrolysis proceeds, WC is protected by the H_2 atmosphere. However, when electrolysis is interrupted, without H_2 protection and an O_2 isolation strategy, the WC becomes oxidized. Since WO_x is formed at the surface of the electrode, the electrolyzer bears a higher cell voltage due to the increase in electronic resistance and activation energy [26]. For a relatively short time after restarting electrolysis, oxidized WC can be reduced, and performance can be self-repaired. After a long time of off electrolysis, oxidization is too serious to be totally recovered. For a short power-off situations, oxidization can be ignored, but part of the oxidized WC is reduced during electrolysis. Compared to the former electrolysis, the WC electrode of the latter operation exhibits H_2 exposure.
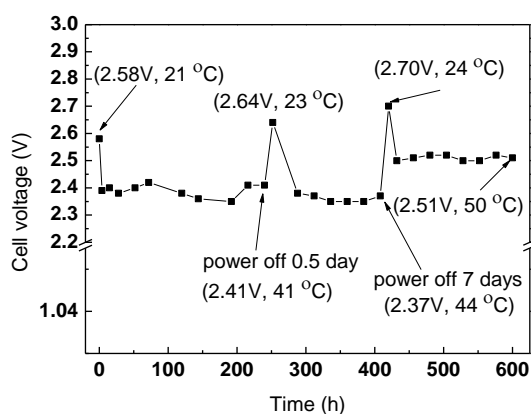

Figure 5. Relationship between cell voltage and time. During electrolysis, the electrolyzer shuts down two times. One stops for 0.5 day and another for 7 days.
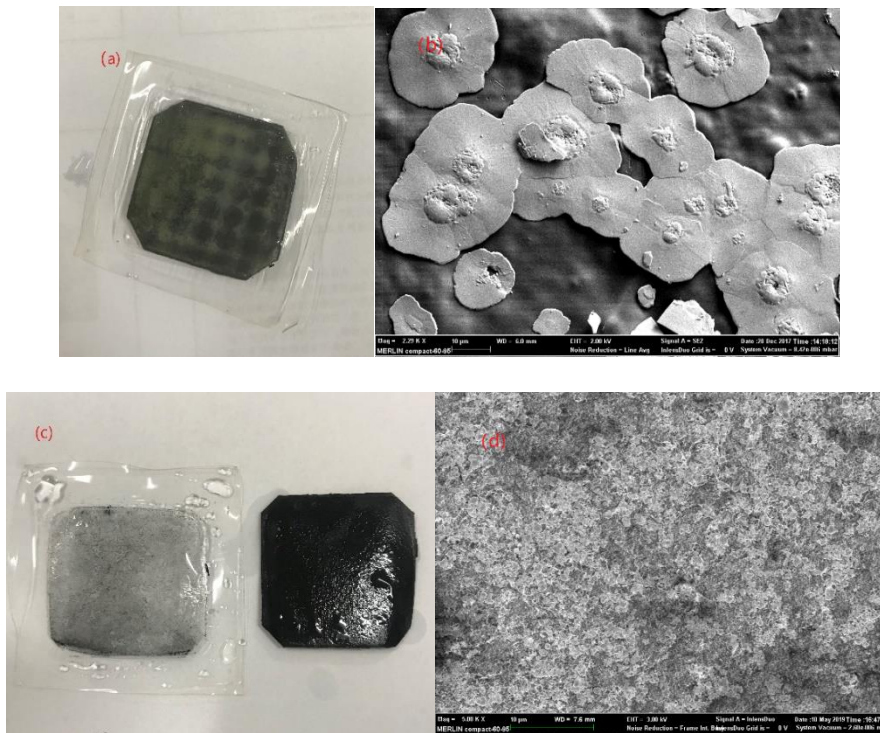
Figure 6. Morphology of WC electrodes. (a) Picture of the WC electrode off-running 15 days. (b) SEM image of the WC electrode off-running 15 days. (c) Picture of the WC electrode off-running. (d) SEM image of the WC electrode off-running.
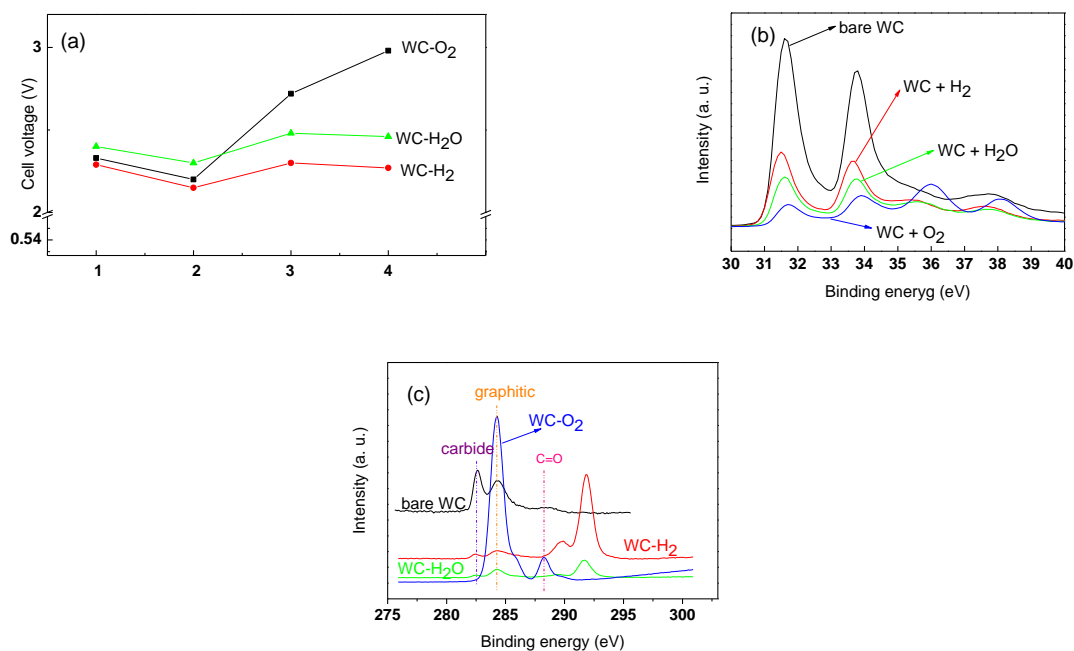
3.4.2 Repair strategy

Figure 7. Performance of the electrolyzer with O_2 exposure and O_2 isolation during inconsecutive electrolysis. Filling O_2, H_2 and H_2O at the cathode chamber when it was in a power-off state. (a) Cell voltage of the electrolyzers. (b) XPS of W4f peaks of the WC electrodes. (c) XPS of C1f peaks of the WC electrodes.

Since the performance loss may be related to the oxidation of WC at power-off operation, the protection strategy of O_2 isolation may be effective, and accelerated tests were performed. Three electrolyzers were prepared and ran for 800 h. During the 4 day power-off electrolysis, one electrolyzer was sealed in pure water in the cathode chamber and the anode water was drained and labelled as WC-H_2O. The other two electrolyzers used H_2 and O_2, respectively, and were, marked as WC-H_2 and WC-O_2. The curve of cell voltage and time is shown in Figure 7(a). When filling the cathode chamber with pure water when the electrolysis was interrupted, the cell voltage of WC-H_2O increased just 30 mV after a four-day restart operation. If H_2 was used as the inlet to the cathode chamber, the performance was better than the initial performance. A climbing cell voltage occurred when O_2 was introduced into the cathode chamber during the power off state.

XPS gives a direct characterization of the surface chemical state. XPS results of the W4f peak (Figure 7(b)) indicates O_2 isolation provided positive results. The $W4f_{7/2}$ and $W4f_{7/2}$ peaks at 31.6 eV and 33.7 eV, respectively, are typical peaks of this commercial WC, while the peaks at 35.8 and 38 eV are typical of WO_3 [32]. Figure 7(c) shows C1s peaks, where the strongest carbide peak of 282.7 eV was detected in bare WC, while a strong graphitic peak was observed in WC-H_2O. XPS gives a direct characterization of the surface chemical state. Graphitic carbon of WC was adverse to the electrochemical activity of HER [11, 27]. The EDX analysis (Table S1) also showed that the H_2-protected electrode showed the lowest atomic ratio of O at the electrode surface.

Despite the fact that the H_2O protection had a 30 mV cell voltage increase, it is an economic and practical solution for industrial consideration, compared with the protection of the consecutive H_2 pumping. Besides, the H_2 strategy was workless with the H_2-sealed method or inletting H_2 from down to up at the cathode chamber. This may be related to poor sealing of the chamber and down-to-up H_2 inletting cannot provide a 100% H_2 atmosphere in the cathode side, and WC can still be oxidized.

WC is widely studied as a promising Pt substitute for HER, as shown in Table 1. However, most of the previous work has shown no investigations on electrolyzer utilization. Besides, the biggest challenge of bara WC is the poor activity and durability. So Pt or other materials have been combined with WC to improve the material which ultimately increase the cost of the electrocatalyst. Developing an electrocatalyst on the nanoscale is a common method to increase the activity, but it also increases the instability risk. Luckily, according to the results above, utilizing WC as an economic HER electrocatalyst is feasible (Figure 8). Although the activity of commercial WC (larger size) is lower than Pt/C, the performance can be improved, as discussed below.

1. Avoiding O_2 exposure, especially in acidic conditions. During operation, WC is protected by the hydrogen atmosphere in the cathode. The oxidization of WC within a short time and without water is not serious. However, when the electrolyzer suffers a long-time power-off without O_2 isolation, WC can become significantly degraded,, the content of noncatalytic graphitic carbon is increased, and the performance drops [27]. Fortunately, oxidation can be protected by full O_2-isolation. Also, H_2-sealing improves the performance.

2. Running at high current density. There are two benefits for high current density operations. First, the cathode chamber is hydrogen-rich, which decreases oxygen dissolution. Second, there is no need to warm the inlet water. The ohmic resistance provides the electrolyzer sufficient heat to run

between 40 - 60 °C. Normally, running at 80 °C is friendly to activation, so it does the proton transfer. Meanwhile, it also accelerates the rate of oxygen dissolution in cathode, which decreases WC stability.

　　　3. Reasonable electrode fabrication methods. Except the electrocatalyst itself, the Nafion ratio, hydrophobic agent composition, and WC loading can all impact the cell voltage of the electrolyzer. Due to relatively poor catalysis for unmodified WC, these factors are not prominent. Activity and stability are still the most important.

Table 1. Summary of WC composites as electrocatalysts for HER and ORR.

Material	Test condition	Electrochemical characterization	References
WC	85% H_3PO_4, 0.1 ~ -2.0 V	WC > Pt, especially running 120 °C to 150 °C	[30]
WC, W_2C	0.5 M H_2SO_4	WC is more Stable	[16][44][45]
WC hollow microspheres	0.5 M H_2SO_4; 0.1 ~ -0.3 V	Pt/WC hs (1223 K) > Pt/WC hs (1273 K) > commercial Pt/C	[25]
WC/CNT	0.5 M H_2SO_4, 0.1 M KOH, 0.1 ~ -0.3 V	WC synthesized at 1050 K had the best performance	[26]
Commercial WC (≤ 1μm)	0.5 M H_2SO_4, -0.15 V ~ -0.25 V	onset overpotential: 0.1 V	This work
WC nanowalls, WC nanocrystalline films	0.5 M H_2SO_4, -0.5 ~ 0.2 V	onset overpotentials: WC nanowalls (-0.052 V), WC nanocrystalline films (-0.102 V)	[27]
3-D porous tungsten-based WS_2 and WC	0.5 M H_2SO_4, 0 ~ -0.3 V	onset overpotentials: WS_2 (100 mV), WC (120 mV)	[24]
WO_3/C	0.5 M H_2SO_4, 1 M KOH	j_o (mA cm^{-2}), 2.0 *10^{-2} (0.5 M H_2SO_4) 5.2 * 10^{-2} (1 M KOH)	[9]
MoS_2, WC/RGO, MoS_2/WC/RGO	0.5 M H_2SO_4, -0.25 ~ 0.05 V	Positive synergistic effect between nano-WC/RGO and layered MoS_2	[4]
W_2C/C, Ag/C, Ag-W_2C/C	1 M KOH	Ag–W_2C/C ≈ Pt/C > Ag/C > W_2C/C	[20]
Pt/C, Pt/WC	0.5 M H_2SO_4, 0.6 ~ 0.8 V	Stable 20 cycles (Pt/C), stable 100 cycles (Pt/WC)	[28][46][47]
Pt-WC/C (intermittent microwave heating),	0.5 M H_2SO_4, 0.0 ~ 1.2 V	Pt-WC/C (intermittent microwave heating) >Pt-WC/C (mechanical mixing) > Pt/C	[22]

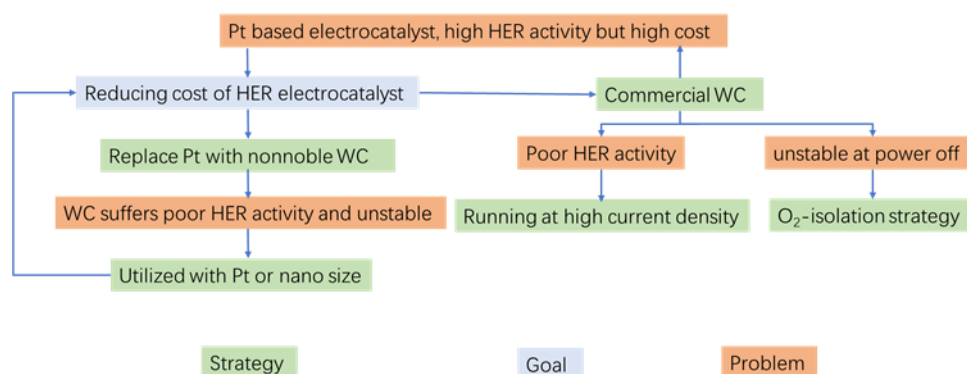|			
Pt-WC/C (mechanical mixing) Pt-W$_2$C/C Pt/C	0.5 M H$_2$SO$_4$, 0.6 ~ 1.2 V	Onset potential: Pt-W$_2$C/C (1.0 V); Pt/C (0.88 V)	[48]
Pt on nano-structured WC	0.5 M H$_2$SO$_4$, 0.05 ~ -0.2 V	Pt/WC (700 K) > Pt/WC (600K) > Pt/WC	[29]
ML Pt-WC, ML Pt-W$_2$C	0.5 M H$_2$SO$_4$, 0 ~ 0.4 V	Pt ≈ ML Pt-WC ≈ ML Pt-W$_2$C	[23]
0.45 ML Pt-WC, 0.65 ML Pt-WC, ML Pt-WC	0.5 M H$_2$SO$_4$	HER activity increased, and ML Pt-WC shared same performance with Pt foil	[17][49]

Figure 8. Schematic of commercial WC as a competitive candidate for HER electrocatalysts for PEMWE.

4. CONCLUSION

Commercial WC as an HER electrocatalyst was investigated. Two sizes of WC were compared, and nanosize WC was found to be unstable for water electrolysis in the electrolyzer. However, most reports have only shown the electrocatalytic performance in a three-electrode system, which does not reflect the real situation of the WC-based electrocatalysts. We fabricated a WC electrode by traditional rolling methods. Some factors impacted the performance during the electrode fabrication process. Removing the solvent by air drying at 130 °C and using mixed hydrophobic agent (3% PTFE + 7% CFx) was preferred. 1.8-2.1 mg cm^{-2} Nafion was brushed on the electrode surface. In addition to the electrode fabrication method, the running condition also affected the performance. Operating at low temperature and high current density was more competitive with Pt/C (Pt 0.2 mg cm^{-2}) electrolysis. Although high temperature benefits HER activity, it also induced instability of the WC electrode. High current density provided higher pressure of H$_2$ at the cathode, creating a reducing atmosphere for WC. It also needed no extra heat to warm the feeding water, because the heat was enough to maintain the temperature at 40-60 °C. Additionally, if no water was supplied at the cathode, the cell voltage would decrease 30 mV due the

increased temperature. However, the WC electrode showed obvious defects, where a non-recoverable performance loss after a long time of off-electrolysis was induced by WC oxidation. Strategies of O_2-isolation and H_2-sealing were effective and showed performance improvements. WC was shown to be an economic replacement for Pt/C for PEMWE applications.

SUPPORTING MATERIAL:

1. Characterization of WC

Commercial WC (Guoyao Reagent, China) was characterized by X-Ray diffraction (XRD, Bruker D8 Advance, Bruker, Germany), Scanning electron microscopy (SEM, Zeiss Merlin Compact, Zeiss, Germany), and X-ray photoelectron spectroscopy (XPS, ESCALAB250Xi, Thermo Fisher Scientific, America). A mixture of 24.5 mg WC, 750 μL deionized water, and 250 μL isopropanol was ultrasonically dispersed for 15 min. Then 5 μL of the aforementioned solution was cast on a well-polished 3 mm diameter glassy carbon electrode (GDE) with a drop of 5 wt% Nafion solution protection. The prepared GDE acted as a working electrode, and a Pt-Ti slice and saturated mercurous sulfate electrode (MSE, 0.652 V *vs*. SHE) were utilized as the counter electrode and reference electrode, respectively. A 2 mol L^{-1} H$_2$SO$_4$ solution was used as the electrolyte. Electrochemical performance was detected with sweep voltammetry (LSV) tests by an electrochemical work station (CHI 660E, Chenhua Instruments Inc. USA). The LSV ran from -0.6 to -0.9 V *vs*. MSE at 2 mV s^{-1} at 25 °C, 40 °C, 60 °C, and 80 °C.

The characterization of WC is shown in Figure S1. The SEM image (Figure S1(a)) indicates that WC shows an average uniform size of 600 nm. The XRD pattern (Figure S1(b)) agreed with the PDF card (51-0939), a typical synthesized WC. LSV results indicated that WC showed higher HER activity at higher temperatures.
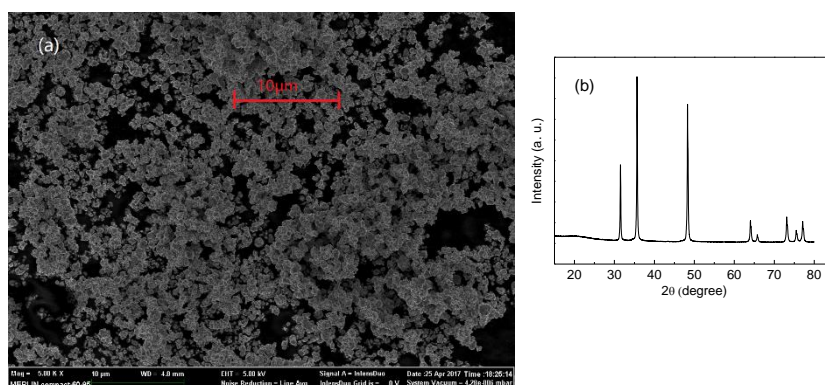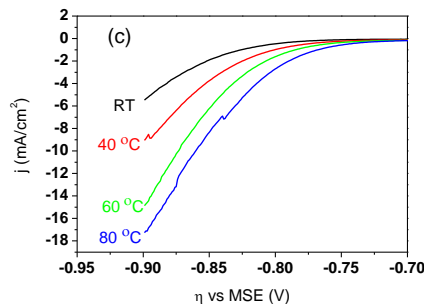
Figure S1 Characterization of WC. (a) SEM image. (b) XRD pattern. (3) LSV curves. WC modified GDE acted as a working electrode, and a Pt-Ti slice and saturated mercurous sulfate electrode (MSE, 0.652 V *vs*. SHE) were utilized as the counter electrode and reference electrode, respectively. A 2 mol L^{-1} H_2SO_4 solution worked as an electrolyte. The LSV ran from -0.6 to -0.9 V *vs*. MSE at 2 mV s^{-1} at 25 °C, 40 °C, 60 °C, and 80 °C.

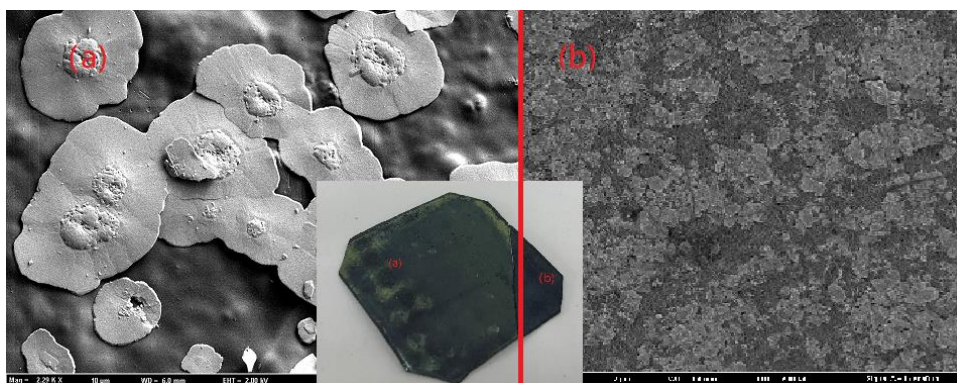## 2. The effects of inconsecutive electrolysis

Figure S2 Images of seriously oxidized WC electrode and a portion of the electrode was oxidized by H_2 for 4 h at room temperature.

Table S1 EDX analysis of WC electrode with a four-day power-off electrolysis, where W and O were analyzed.

Atom ratio (%)	WC-H_2	WC- H_2O	WC- O_2
W	83.7	74.4	51.0
O	16.3	25.6	49.0

Table S2 XPS of WC electrodes with a four-day power-off electrolysis.

Peaks (eV)	WC-H_2	WC-O_2	WC-H_2O
C1s	291.9	284.3	291.7
O1s	530.4	530.9	530.9
W4f	31.5	36.0	31.6

References

1. P. Millet, R. Ngameni, S. A. Grigoriev and V. N. Fateev, *Int. J. Hydrogen Energy,* 36 (2011) 4156.
2. I. Dedigama, P. Angeli, N. Dijk, J. Millichamp, D. Tsaoulidis, P. R. Shearing and D. J. L. Brett, *J. Power Sources,* 265 (2014) 97.
3. M. Y. Wang, Z. Wang, X. Gong and Z. C. Guo, *Renew. Sust. Energy Rev.,* 29 (2014) 573.
4. B. Han, S. M. Steen III, J. K. Mo and F. Y. Zhang, *Int. J. Hydrogen Energy,* 40 (2015) 7006.
5. M. Carmo, D. L. Fritz, J. Merge and D. Stolten, *Int. J. Hydrogen Energy,* 38 (2013) 4901.
6. S. Siracusanoa, N. V. Dijk, E. Payne-Johnson, V. Baglio and A. S. Aricò, *Appl. Catal. B-Environ.,* 164 (2015) 488.
7. C. Rozain, E. Mayousse, N. Guillet and P. Millet, *Appl. Catal. B-Environ.,* 182 (2016) 123.
8. J. Y. Xu, G. Y. Liu, J. L. Li and X. D. Wang, *Electrochimi. Acta,* 59 (2012) 105-112.
9. H. T. Zheng and M. Mathe, *Int. J. Hydrogen Energy,* 36 (2011) 1960.
10. Y. Hara, N. Minami, H. Matsumoto and H. Itagaki, *Appl. Catal. A-Gen.,* 332 (2007) 289.
11. F. Harnisch, U. Schröder, M. Quaas and F. Scholz, *Appl. Catal. B-Environ.,* 87 (2009) 63-69.
12. E. C. Weigert, A. L. Stottlemyer, M. B. Zellner and J. G. Chen, *J. Phys. Chem. C,* 111 (2007) 14617.
13. G. F. Cui, P. K. Shen, H. Meng, J. Zhao and G. Wu, *J. Power Sources,* 196 (2011) 6125.
14. D. J. Ham, Y. K. Kim, S. H. Han and J. S. Lee, *Catal. Today*, 132 (2008) 117.
15. K. Lee, A. Ishihara, S. Mitsushima, N. Kamiya and K. Ota, *Electrochimi. Acta,* 49 (2004) 3479.
16. M. B. Zellner and J. G. Chen, Cataly. Today, 99 (2005) 299.
17. D. V. Esposito, S. T. Hunt, A. L. Stottlemyer, K. D. Dobson, B. E. McCandless, R. W. Birkmire and J. G. Chen, *Angew. Chem. Int. Ed.,* 49 (2010) 9859.
18. F. Harnisch, G. Sievers and U. Schröder, *Appl. Catal. B-Environ.,* 89 (2009) 455.
19. R. D. Armstrong and M. F. Bell, *Electrochimi. Acta,* 23 (1978) 1111.
20. Y. Yan, B. Y. Xia, X. Y. Qi, H. B. Wang, R. Xu, J. Y. Wang, H. Zhang and X. Wang, *Chem. Commun.,* 49 (2013) 4884.
21. H. Meng and P. K. Shen, *Electrochem. Commun.,* 8 (2006) 588.
22. M. Nie, P. K. Shen, M. Wu, Z. D. Wei and H. Meng, *J. Power Sources,* 162 (2006) 173.
23. D. V. Esposito, S. T. Hunt, Y. C Kimmel and J. G. Chen, *J. Am Chem Soc.,* 134 (2012) 3025-3033.
24. H. Fei, Y. Yang, X. Fan, G. Wang, G. Ruan and J. M. Tour, *J. Mater. Chem. A,* 3 (2015) 5798.
25. C. Tang, D. Wang, Z. Wu and B. Duan, *Int. J. Hydrogen Energy,* 40 (2015) 3229.
26. X. Fan, H. Zhou and X. Guo, *ACS Nano,* 9 (2015) 5125.
27. Y. Ko, J. Cho, I. Kim, D. S. Jeong, K. Lee, J. Park, Y. Baik, H. Choi and W. Lee. *Appl. Catal. B-Environ.,* 203 (2017) 684.
28. Y. C. Kimmel, D. V. Esposito, R. W. Birkmire and J. G. Chen. *Int. J. Hydrogen Energy,* 37 (2012) 3019.
29. C. Liu, D. Zhou, J. Zhou, Z. Xie and Y. Xia, *RSC Adv.* 6 (2016) 76307.
30. A. V. Nikiforov, I. M. Petrushina, E. Christensen, N. V. Alexeev, A. V. Samokhin and N. J. Bjerrum, *Int. J. Hydrogen Energy,* 37 (2012) 18591
31. C. A. Ma, W. K. Zhang, D. H. Chen and B. X. Zhou, *Trans. Nonferrous Met. Soc. China* 12 (2002) 1015.
32. F. Harnisch, U. Schröder, M. Quaas and F. Scholz, *Appl. Catal. B-Environ.,* 87 (2009) 63
33. Y. Y. Shao, J. Liu, Y. Wang and Y. H. Lin, *J. Mater. Chem.,* 19 (2009) 46
34. Y. Liu, T. G. Kelly, J. G. Chen and W. E. Mustain, *ACS Cataly.,* 3 (2013) 1184
35. D. V. Esposito and J. G. Chen, *Energy Environ. Sci.,* 4 (2011) 3900
36. S. S. Chen, F. L. Jiang, X. F. Xie, Y. Q. Zhou and X. H. Hu, *Electrochimi. Acta,* 192 (2016) 357
37. W. F. Chen, J. T. Muckerman and E. Fujita, *Commun.,* 49 (2013) 8896
38. L. Xing, W. Shi, H. Su, Q. Xu, P. K. Das, B. Mao and K. Scott, *Energy,* 177 (2019) 445
39. D. S. Hwang, C. H. Parka, S. C. Yi and Y. M. Lee, *Int. J. Hydrogen Energy,* 36 (2011) 9876.

40. X. Cheng, B. Yi, M. Han, J. Zhang, Y. Qiao and J. Yu, *J. Power Sources,* 79 (1999) 75-81.
41. G. Jeong, Mi. J. Kimc, J. Hand, H. Kim, Y. Shul and E. A. Cho, *J. Power Sources,* 323 (2016) 142.
42. K. Shinozaki, Y. Morimoto, B. S. Pivovar and S. S. Kocha, *J. Power Sources,* 325 (2016) 745.
43. H. Liang, H. Su, B. G. Pollet and S. Pasupathi, *J. Power Sources,* 288 (2015) 121.
44. S. Shahgaldi, I. Alaefour, G. Unsworth and X. Li, *Int. J. Hydrogen Energy,* 42 (2017) 11813
45. M. C. Weidman, D. V. Esposito, Y. Hsu and J. G. Chen, *J. Power Sources,* 202 (2012) 11.
46. E. C. Weigert, D. V. Esposito and J. G. Chen, *J. Power Sources,* 193 (2009) 501.
47. H. Chhina, S. Campbell and O. Kesler, *J. Power Sources,* 164 (2007)431
48. Y. Liu andW. E. Mustain, *Int. J. Hydrogen Energy,* 37 (2012) 8929
49. H. Meng and P. K. Shen, *J. Phys. Chem. B,* 109 (2005) 22705